2010 21st International Lightning Detection Conference
19 – 20 April • Orlando, Florida, USA
3rd International Lightning Meteorology Conference
21 – 22 April • Orlando, Florida, USA

COMPACT INTRACLOUD DISCHARGES: ON ESTIMATION OF PEAK CURRENTS FROM MEASURED ELECTROMAGNETIC FIELDS

Amitabh Nag[1], Vladimir A. Rakov[1], and John A. Cramer[2]
[1] Department of Electrical and Computer Engineering, University of Florida, Gainesville, Florida, USA
[2] Vaisala Inc., Tucson, Arizona, USA

Abstract: Using measured wideband electric field waveforms and the Hertzian dipole (HD) approximation, we estimated peak currents for 48 located compact intracloud lightning discharges (CIDs). CID channel lengths are expected to range from about 100 to 1000 m and in many cases can be considered electrically short. The fields were measured at the Lightning Observatory in Gainesville (LOG), Florida. Horizontal distances to the sources were reported by the NLDN, and source heights were estimated from the ratio of electric and magnetic (also measured at the LOG) fields. The 48 CIDs were reported by 4 to 22 (11 on average) NLDN sensors and were correctly identified by the NLDN as cloud discharges. The majority of NLDN-reported peak currents are considerably smaller than those predicted by the HD approximation. Some discrepancy is expected because NLDN-reported peak currents are assumed to be proportional to peak fields, which is a reasonable approximation for return strokes, while for the HD approximation the peak of electric or magnetic radiation field component is proportional to the peak of current time derivative (d*i*/dt). The results of this study have important implications for estimation of peak currents for cloud discharges.

1. Introduction

Cloud lightning discharges that produce both (1) single, usually solitary bipolar electric field pulses having typical full widths of 10 to 30 μs and (2) intense HF-VHF radiation bursts (much more intense than those from any other cloud-to-ground or "normal" cloud discharge process) are referred to as Compact Intracloud Discharges (CIDs). These discharges were first reported by *Le Vine* [1980] and later characterized by *Willett et al.* [1989], *Smith et al.* [1999], *Eack* [2004], *Hamlin et al.*, [2009], and *Nag et al.* [2009] among others. Most of the reported electric field signatures of these discharges are produced by distant (tens to hundreds of kilometers) events and hence are essentially radiation. The radiation field pulses produced by CIDs are sometimes referred to as Narrow Bipolar Pulses (NBPs). CIDs tend to occur at high altitudes (greater than 10 km) and have relatively short channel lengths of 100 to 1000 m. Many of them are expected to be electrically short radiators (shorter than the shortest significant excitation wavelength).

We used the vertical Hertzian dipole approximation to estimate peak currents of 48 located CIDs from their measured electric fields. The majority of NLDN-reported peak currents for these CIDs are considerably smaller than those predicted by the Hertzian dipole approximation. In this paper, we examine the reasons for this discrepancy.

2. Data

Data for the 48 CIDs examined here were acquired in August-September of 2008 at the Lightning Observatory in Gainesville (LOG), Florida. The electric field measuring system included an elevated circular flat-plate antenna followed by an integrator and a unity-gain, high-input-impedance amplifier. The system had a useful frequency bandwidth of 16 Hz to 10 MHz, the lower and upper limits being determined by the RC time constant (about 10 ms) of the integrator and by the amplifier, respectively. The wideband magnetic field (B), which was used in estimating the source height, was obtained by integrating and combining the two orthogonal components of dB/dt. The dB/dt measuring system employed two orthogonal loop antennas, each followed by an amplifier. The upper frequency response of the dB/dt measuring system was 15 MHz. All the antennas were installed on the roof of a five-storey building. Fiber-optic links were used to transmit the field and field-derivative signals from the antennas and associated electronics to an 8-bit digitizing

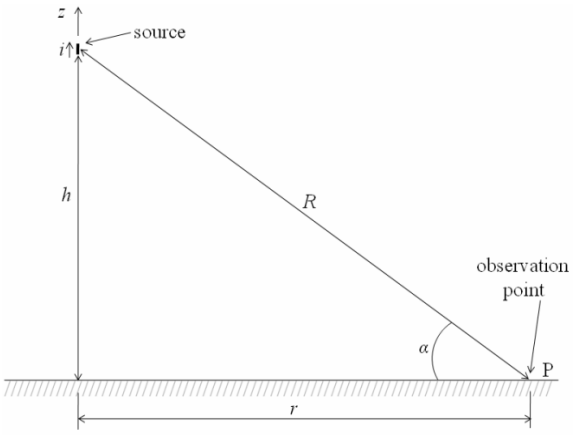

Figure 1. Geometrical parameters needed in calculating the vertical electric field at observation point P on perfectly conducting ground at horizontal distance r from a vertical Hertzian dipole representing the CID channel.

oscilloscope which digitized the signals at 100 MHz. The record length was 500 ms including pre-trigger time of 100 ms. CIDs were identified by their intense VHF radiation signature (also recorded at the LOG) and characteristic wideband field and field derivative waveforms.

GPS timestamps were used to identify CIDs recorded at the LOG in the National Lightning Detection Network (NLDN) records. NLDN-estimated horizontal distances from the 48 CIDs to the LOG varied from 12 to 89 km. The CIDs were each reported by 4 to 22 (11 on average) NLDN sensors, although the maximum number of sensors used in the final location calculation was 10 [*Cummins*, personal communication, 2010]. The semi-major axis lengths of 50% location error ellipse ranged from 400 m to 4.9 km (mostly 400 m, so that the median was as small as 400 m).

Simultaneous measurements of electric and magnetic radiation field pulses produced by the 48 CIDs and corresponding NLDN-reported horizontal distances were used to estimate source heights [*Nag et al.,* 2009]. The minimum and maximum source heights were 8.8 and 29 km, respectively. The geometric mean was 16 km and median was 15 km, the latter being similar to the median source height of 13 km reported for the same CID wideband electric field initial polarity by *Smith et al.* [2004]. The overall error in height estimates ranged from 4.7 to 95% with a mean of 17%. If 9 events with height errors greater than 25% were excluded, the geometric mean height would remain the same as that for the original sample of 48. The height errors appear to be independent of the height value, and the larger height errors have not contributed significantly to the errors in peak currents.

3. Estimation of CID Currents Using the Hertzian Dipole Approximation

A dipole can be viewed as Hertzian or electrically short if its length Δh is very short compared to the shortest significant excitation wavelength λ. For example, a dipole of length, Δh = 500 m can be considered Hertzian if λ>>500 m. This means that the Hertzian dipole (HD) approximation is valid for frequencies f << 600 kHz. *Nag* [2010] showed that the HD approximation should be valid for a large subset of combinations of CID parameters.

Let us consider a vertical Hertzian dipole of length Δh at height h above perfectly conducting ground carrying a uniform current *i(t)* (see Figure 1). The total electric field at the observation point P on the ground at a horizontal distance r is given by:

$$E_z(r,t) = \frac{1}{2\pi\varepsilon_0}\left[\frac{(2h^2 - r^2)\Delta h}{R^5}\int_0^t i(\tau - R/c)\,d\tau + \frac{(2h^2 - r^2)\Delta h}{cR^4} i(t - R/c) - \frac{r^2 \Delta h}{c^2 R^3}\frac{di(t - R/c)}{dt}\right] \quad (1)$$

where ε_0 is the electric permittivity of free space, c is the free-space speed of light, and R is the inclined distance from the dipole to the observation point, which is given by $R = \sqrt{h^2 + r^2}$. Note that current i in Equation (1) varies only as a function of time, with all the geometrical parameters being fixed.

Equation (1) can be rewritten as a second order differential equation:

$$\frac{dE_z}{dt} = \frac{\Delta h}{2\pi\varepsilon_0}\left[\frac{(2h^2 - r^2)}{R^5} i + \frac{(2h^2 - r^2)}{cR^4}\frac{di}{dt} - \frac{r^2}{c^2 R^3}\frac{d^2 i}{dt^2}\right] \quad (2)$$

where arguments of E_z and i have been dropped to simplify notation. For known E_z and the geometrical parameters (Δh, h, and r) this equation can be numerically solved for i.

We employed the Runge-Kutta method of order three (with four stages and an embedded second-order method, also known as the Bogacki–Shampine method [*Bogacki and Shampine*, 1989]) to solve Equation (2) for i using measured electric fields E_z of the 48 CIDs with known h and r. The initial and final values of current were required to be zero, and the error tolerance of the numerical solution was set to 10^{-6}.

Channel lengths Δh for 9 of the 48 CIDs were estimated from reflections in electric field derivative (dE/dt) waveforms (also measured at the LOG) and assumed propagation speed of 2.5 x 10^8 m/s. For the remaining 39 CIDs there were no reflection signatures observed, and a reasonable value of Δh = 350 m was assumed. This value is consistent with the Hertzian dipole approximations for speeds in the range of 2 to 3 x 10^8 m/s [*Nag*, 2010].

For E_z measured at far distances, the peak current can also be estimated using the radiation field approximation, given by the third term of Equation (2):

$$\frac{dE_z}{dt} = -\frac{\Delta h r^2}{2\pi\varepsilon_0 c^2 R^3}\frac{d^2 i}{dt^2}, \qquad (3)$$

from which it follows that E_z is proportional to $\frac{di}{dt}$:

$$E_z = -\frac{\Delta h r^2}{2\pi\varepsilon_0 c^2 R^3}\frac{di}{dt}. \qquad (4)$$

In contrast, for distant lightning return strokes represented by the transmission line (TL) model [*Uman and McLain*, 1969] E_z is proportional to i:

$$E_z = -\frac{v}{2\pi\varepsilon_0 c^2 r} i, \qquad (5)$$

where v is the return-stroke propagation speed. Equation (5) is valid when (i) the height above ground of the upward-moving return stroke front is much smaller than the distance r between the observation point on ground and channel base, so that all contributing channel points are essentially equidistant from the observer, (ii) v = constant, (iii) the return-stroke front has not reached the top of the channel, and (iv) the ground conductivity is high enough that propagation effects are negligible. The corresponding magnetic radiation field can be found from $|B_\varphi| = |E_z|/c$.

The apparent discrepancy between Equations (4) ($E_z : \frac{di}{dt}$) and (5) ($E_z : i$) is because of (a) integration over height z (over many electrically short dipoles) that is involved in derivation of Equation (5) and (b) direct proportionality between the time and spatial derivatives of current ($\frac{\partial i}{\partial t} = -v\frac{\partial i}{\partial z}$) predicted by the TL model, on which Equation (5) is based.

The CID currents based on the HD approximation are affected by the errors in heights and in NLDN-estimated horizontal distances. We estimated that the errors in currents due to errors in heights and horizontal distances were less than 15% for 47 of the 48 CIDs (including those with height errors greater than 25%) and for one CID (which had an unusually large horizontal distance error of 21%) the error in current was 23%.

Perhaps the largest uncertainty in our current estimates is due to the uncertainty in Δh. For 9 events with channel lengths estimated from channel traversal times (reflection signatures in dE/dt waveforms) for the assumed v = 2.5 x 10^8 m/s, the uncertainty in current is ≤ 25% [*Nag*, 2010]. For the remaining 39 events, which did not exhibit reflection signatures and for which the channel length was assumed to be 350 m, we cannot assign any specific uncertainty (which is expected to be larger than that for the 9 events discussed above) to the estimated currents. However, we will see in Section 5 that the 9- and 39-event data subsets exhibit similar trends.

4. Estimation of Peak Currents by the NLDN

The NLDN outputs a peak current estimate for each stroke using the measured magnetic radiation field peaks and distances to the ground strike point reported by multiple sensors. The

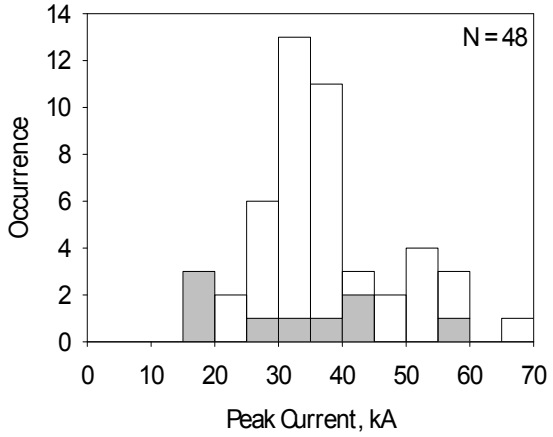

	CIDs with reflection signatures	CIDs without reflection signatures	All CIDs
AM, kA	33	38	37
GM, kA	31	36	35
Min, kA	18	21	18
Max, kA	60	67	67
N	9	39	48

Figure 2. Histogram of NLDN-estimated peak currents for 48 CIDs. Statistics given are the arithmetic mean (AM), geometric mean (GM), minimum value (Min), and maximum value (Max) for the 9 (with reflection signatures) and 39 (without reflection signatures) events individually and for all data combined.

following field-to-current conversion equation is used:

$$i_p = 0.185\ Mean(RNSS), \qquad (6)$$

where i_p is the peak current in kA and *Mean(RNSS)* is the mean of range–normalized (to 100 km) signal strengths, in so-called LLP units, from all sensors allowed by the central analyzer to participate in the peak current estimate. Generally, contributions from sensors at distances up to several hundreds of kilometers are included. Equation (6) implies that the magnetic (as well as electric) radiation field is proportional to the current, similar to Equation (5).

Normalization of measured signal strength, SS, to 100 km is performed taking into account signal attenuation due to its propagation over lossy ground. The following empirical formula has been used to compensate for propagation effects since 2004:

$$RNSS = SS(\frac{r}{100})\exp(\frac{r-100}{1000}), \qquad (7)$$

where r is in kilometers and SS is in LLP units. This equation assumes that the distance dependence of signal strength is $r^{-1}\exp(\frac{-r}{1000})$, where r^{-1} corresponds to propagation over perfectly conducting ground and $\exp(\frac{-r}{1000})$ represents additional attenuation due to ground being lossy. The exponential function in Equation (7) should increase the *RNSS* in order to compensate for propagation effects. For r = 625 km, for example, it is equal to 1.7, although for r ranging from 0 to 100 km it varies from about 0.9 to 1.

The median value of absolute current estimation error for negative subsequent strokes was found, using rocket-triggered lightning data, to be 20% with a maximum of 50% [*Jerauld et al.,* 2005; *Nag et al.,* 2008]. No current error estimates are available for first strokes or for cloud discharges.

5. Analysis and Discussion

Histogram of NLDN-reported peak currents for 48 CIDs is shown in Figure 2. The peak currents range from 18 to 67 kA with the geometric (GM) value being 35 kA. Histogram of peak currents estimated using the Hertzian dipole approximation for the same 48 CIDs is shown in Figure 3. The peak currents range from 33 to 259 kA with the GM value being 74 kA. The latter is about a factor of 2.1 larger than the GM based on NLDN data. Figure 4 shows a scatter plot of the NLDN-reported peak current versus peak current estimated using the HD approximation.

As seen in Fig. 4, the majority of NLDN-reported peak currents are considerably smaller than those predicted by the HD approximation. Some discrepancy is expected because NLDN-reported peak currents are assumed to be proportional to peak fields, which is a reasonable approximation for return strokes, but not for electrically short radiators, while for the HD approximation the peak of electric or

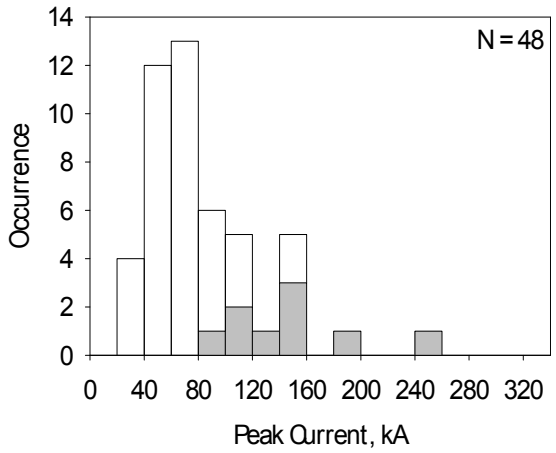

	CIDs with reflection signatures	CIDs without reflection signatures	All CIDs
AM, kA	150	69	84
GM, kA	143	64	74
Min, kA	87	33	33
Max, kA	259	160	259
N	9	39	48

Figure 3. Histogram of peak currents estimated for 48 CIDs using Equation 2. For 9 events with reflection signatures, channel lengths were inferred using channel traversal times measured in dE/dt waveforms and assumed propagation speed of 2.5 x 10^8 m/s. For the other 39 events an assumed channel length of 350 m (implied v ≥ 2 x 10^8 m/s) was used. Statistics given are the arithmetic mean (AM), geometric mean (GM), minimum value (Min), and maximum value (Max) for the 9 and 39 events individually and for all data combined.

magnetic radiation field component is proportional to the peak of the time derivative of current ($\frac{di}{dt}$) (see Equation (4)). It follows that the CID current peak is proportional to the peak of the integral of electric or magnetic radiation field, which occurs at the time of field zero-crossing. In order to examine this discrepancy further, we computed CID peak currents using our measured electric field peaks and Equation (5) with v = 1.8 x 10^8 m/s. This value of speed was used because it had provided a good match between NLDN-reported peak currents and those estimated using the TL model for negative first and subsequent return strokes recorded at the LOG [*Nag*, 2010]. Thus, these calculations, assuming direct proportionality between *i* and E_z, simulate, to some extent, NLDN peak current estimates. The results are shown in Figure 5. Clearly, the discrepancy between the predictions of Equation (5) and NLDN-reported values is appreciably smaller than that between the predictions of Equation (4) and NLDN estimates (the ratio of GM values in the former case is 1.2 versus 2.1 in the latter). However, there seem to be some factors that make NLDN-reported currents smaller than their counterparts based on Equation (5).

One of these factors can be field attenuation due to its propagation over lossy ground. It is seen in Figure 5 that the discrepancy tends to increase with increasing the peak current. Events with larger peak currents are reported by a larger number of NLDN sensors and, hence, their NLDN-reported currents are more influenced by more strongly attenuated contributions from distant sensors. The NLDN current estimation procedure does include compensation for the field propagation effects (see Equation (7)). However, if this compensation is not sufficient, the NLDN-reported peak current will be an underestimate. As noted in Section 2, the 48 CIDs were reported by 4 to 22 (11 on average) NLDN stations, so that contributions from distances up to several hundreds of kilometers could be included, while the distances for our estimates based on Equation (5) were considerably smaller, ranging from 12 to 89 km.

It is worth noting that most of the peak current estimates based on the HD approximation cannot be viewed as ground-truth data, due to uncertainties in the model input parameters. While for the 9 events with channel lengths estimated from channel traversal times those uncertainties are up to 25%, they are much larger for the other 39 events (see Section 3). Note, however, that the two data subsets exhibit similar trends (see Figures 4 and 5)

6. Summary

CIDs tend to occur at high altitudes (greater than 10 km) and have relatively short channel lengths of 100 to 1000 m. Many of them are expected to be electrically short radiators (shorter than the shortest significant excitation wavelength). We estimated peak currents for 48 located CIDs using measured wideband electric

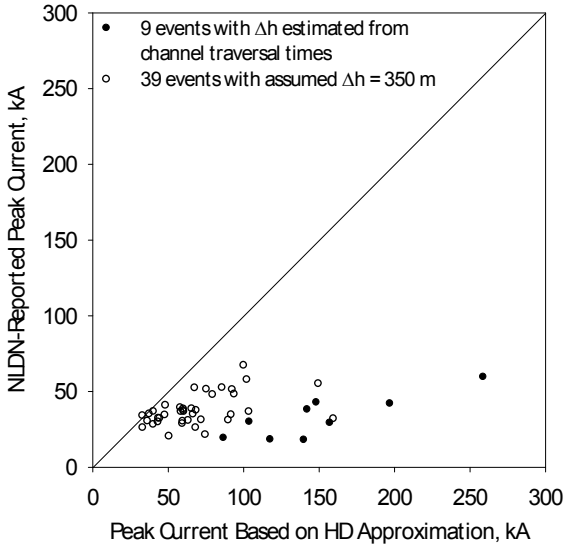

Figure 4. NLDN-reported peak current versus peak current estimated using the Hertzian dipole (HD) approximation for 48 CIDs. For 9 events (solid circles), channel lengths were inferred using channel traversal times measured in dE/dt waveforms and assumed propagation speed of 2.5 x 10^8 m/s. For the other 39 events (hollow circles) an assumed channel length of 350 m (with implied v ≥ 2 x 10^8 m/s) was used.

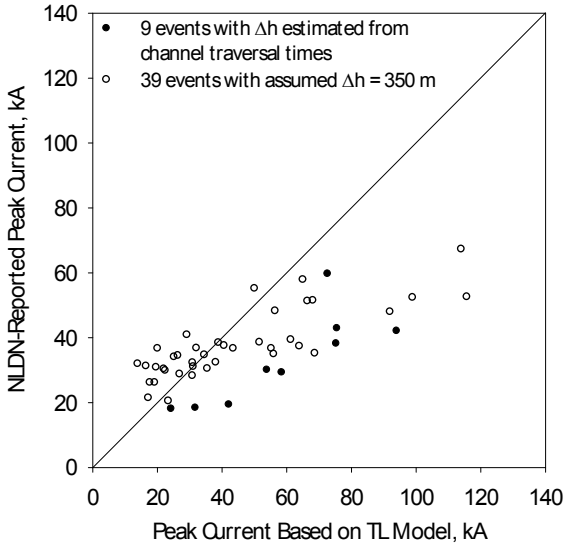

Figure 5. NLDN-reported peak current versus peak current estimated using Equation 4 with v = 1.8 x 10^8 m/s for 48 CIDs. Hollow and solid circles represent the two subsets of events identified in the caption of Figure 4.

field waveforms and the Hertzian (electrically short) dipole approximation. The majority of NLDN-reported peak currents for these CIDs are considerably smaller than those predicted by the HD approximation. Some discrepancy is expected because NLDN-reported peak currents are assumed to be proportional to peak fields, which is a reasonable approximation for return strokes, while for the HD approximation the peak of electric radiation field is proportional to the peak of the time derivative of current ($\frac{di}{dt}$). It follows that the CID current peak is proportional to the peak of the integral of electric or magnetic radiation field, which occurs at the time of field zero-crossing. Additionally, undercompensated field attenuation due to its propagation over lossy ground could have contributed to the discrepancy.

It is worth noting that most of the peak current estimates based on the HD approximation cannot be viewed as ground-truth data, due to uncertainties in the model input parameters. While for the 9 events with channel lengths estimated from channel traversal times those uncertainties are up to 25%, they are much larger for the other 39 events (see Section 3). However, these two data subsets exhibit similar trends.

The results of this study have important implications for estimation of peak currents for cloud discharges [e.g., this study and *Betz et al.*, 2009]. If radiator is short, as in the case of CIDs, the field-to-current conversion procedure designed for return strokes, in which the current is directly proportional to the field, may yield incorrect results.

References

Betz, H.-D., K. Schmidt, and W.P. Oettinger (2009), LINET - An international VLF/LF lightning detection network in Europe, In *Lightning: Principles, Instruments and Applications*, eds. H.-D. Betz, U. Schumann, and P. Laroche, Springer-Verlag, New York.

Bogacki, P., and L.F. Shampine (1989), A 3(2) pair of Runge–Kutta formulas, *Applied Mathematics Letters 2* (4): 321–325, doi:10.1016/0893-9659(89)90079-7.

Eack, K. B. (2004), Electrical characteristics of narrow bipolar events, *Geophys. Res. Lett., 31*, L20102, doi:10.1029/2004GL021117.

Hamlin, T., K. C. Wiens, A. R. Jacobson, T. E. L. Light, and K. B. Eack (2009), Space- and ground-based studies of lightning signatures, in *Lightning: Principles, Instruments and Applications*, eds. H.-D. Betz, U. Schumann, and P. Laroche, New York: Springer-Verlag, pp. 287–307.

Jerauld, J., V. A. Rakov, M. A. Uman, K. J. Rambo, D. M. Jordan, K. L. Cummins, and J. A. Cramer (2005), An evaluation of the performance characteristics of the U.S. National Lightning Detection Network in Florida using rocket-triggered lightning, *J. Geophys. Res., 110*, D19106, doi:10.1029/2005JD005924.

Le Vine, D. M. (1980), Sources of the strongest RF radiation from lightning, *J. Geophys. Res., 85,* 4091-4095.

Nag, A. (2010), Characterization and modeling of lightning processes with emphasis on compact intracloud discharges, Ph.D. dissertation, University of Florida, May 2010.

Nag, A., J. Jerauld, V.A. Rakov, M.A. Uman, K.J. Rambo, D.M. Jordan, B.A. DeCarlo, J. Howard, K.L. Cummins, and J.A. Cramer (2008), NLDN responses to rocket-triggered lightning at Camp Blanding, Florida, in 2004 and 2005, *29th International Conference on Lightning Protection*, paper no. 2–05, Uppsala, Sweden.

Nag, A., and V.A. Rakov (2009), Compact intracloud lightning discharges: conceptual mechanism, modeling, and electrical parameters, Abstract AE32A-01, *American Geophysical Union Fall Meeting*, San Francisco.

Nag, A., V. A. Rakov, D. Tsalikis, and J. A. Cramer (2009), Intense electromagnetic radiation from cloud lightning discharges, *X International Symposium on Lightning Protection, Curitiba, Brazil, November*, 2009.

Smith, D. A., M. J. Heavner, A. R. Jacobson, X. M. Shao, R. S. Massey, R. J. Sheldon, and K. C. Weins (2004), A method for determining intracloud lightning and ionospheric heights from VLF/LF electric field records, *Radio Sci., 39*, RS1010, doi:10.1029/2002RS002790.

Smith, D. A., X. M. Shao, D. N. Holden, C. T. Rhodes, M. Brook, P. R. Krehbiel, M. Stanley, W. Rison, and R. J. Thomas (1999), A distinct class of isolated intracloud discharges and their associated radio emissions, *J. Geophys. Res., 104*, 4189–4212.

Uman, M. A., and D. K. McLain (1969), Magnetic field of the lightning return stroke, *J. Geophys. Res.*, *74*, 6899–6910.